

8. Halliday, D., Resnick, R. and Walker, J., In *Fundamentals of Physics*, John Wiley, New York, 2001, 6th edn.
9. Stoner, E. C., Atomic moments in ferromagnetic metals and alloys with non-ferromagnetic elements. *Philos. Mag.*, 1933, **15**, 1018.
10. Mott, N. F. and Stevens, K. W. H., The band structure of the transition metals. *Philos. Mag.*, 1957, **2**, 1364–1386.
11. Crangle, J., The magnetic moments of cobalt–copper alloys. *Proc. R. Soc., London, Ser. 7*, 1955, **46**, 499–516.
12. Vogt, E., In *Magnetism and Metallurgy* (eds Berkowitz, A. E. and Kneller, E.), Academic Press, New York, 1969, pp. 249–328.
13. King, H. W., Quantitative size factors for metallic solid solutions. *J. Mater. Sci.*, 1966, **1**, 79–90.
14. Bhatia, M. L., Singh, A. K. and Nandy, T. K., Volume size factor and lattice parameter in cubic intermetallics with LI_2 structure. *Intermetallics*, 1996, **4**, 635–639.
15. Bhatia, M. L., Singh, A. K. and Nandy, T. K., Volume size factor and lattice parameter in cubic intermetallics with B2 structure. *Intermetallics*, 1998, **6**, 141–146.
16. Bhatia, M. L., Volume of formation and ligand field effects in some intermetallics. *Intermetallics*, 1999, **7**, 641.
17. Balkis, K., Ameen and Bhatia, M. L., Stability regime of $CaCu_5$ structure. *J. Alloy. Compound.*, 2001, **123**, 1039–1045.
18. Bhatia, M. L., On the packing of $AuCu_3$ and Cu_2Mg structures. *Philos. Mag.*, 2003, **83**, 2293–2300.
19. Bhatia, M. L. and Cahn, R. W., The anomalous contraction on disordering Ni_3Si . *Intermetallics*, 2003, **11**, 673–676.
20. Bhatia, M. L. and Cahn, R. W., Lattice parameter changes on disordering. *Intermetallics*, 2005, **13**, 474–483.
21. Schlosser, W. F., Magnetic contribution to atomic volume of d group transition metals. *J. Magn. Magn. Mater.*, 1976, **1**, 102–105.
22. Schlosser, W. F., Magnetic contribution to the atomic volume in alloys of Fe, Mn and Cr. *J. Magn. Magn. Mater.*, 1976, **1**, 293–304.
23. Schlosser, W. F., Magnetic contribution to the atomic volume of Co, Fe, Mn and Fe–3d metal alloys. *J. Magn. Magn. Mater.*, 1975, **1**, 106–113.
24. Schlosser, W. F., Calculation of atomic volume of Fe–Ni and Fe–Co alloys. *Phys. Stat. Sol.*, 1973, **17**, 199–205.
25. Schwarz, K., Mohn, P., Blaha, P. and Kubler, J., Electronic and magnetic structure of BCC Fe–Co alloys from band theory. *J. Phys. F*, 1984, **14**, 2659–2671.
26. Hara, Y., Handley, R. C. O. and Grant, N. J., Magnetic properties of $Mn_{1-x}Ni_xAl$. *J. Magn. Magn. Mater.*, 1986, **54**, 1077–1078.
27. Williams, D. E. G. and Jezierski, A., Magnetic order in crystallographically ordered $Pt_{4-y}(Mn_xCr_{1-x})_y$ alloys. *J. Magn. Magn. Mater.*, 1986, **59**, 41–56.
28. Irshikawa, H. *et al.*, Atomic ordering and magnetic properties in $Ni_2Mn(Ga_xAl_{1-x})$ Heusler alloys. *Acta Mater.*, 2008, **56**, 4789–4797.
29. Arp, V., Edmonds, D. and Petersen, R., Hyperfine coupling in CoFe and CoNi alloys as determined by heat capacity measurements. *Phys. Rev. Lett.*, 1959, **3**, 5.
30. Cheng, C. H., Wei, C. T. and Beck, P. A., Low-temperature specific heat of body-centered cubic alloys of 3d transition elements. *Phys. Rev.*, 1960, **120**, 426–436.

ACKNOWLEDGEMENTS. I thank Prof. K. P. Abraham for teaching me the basics of metallurgical thermodynamics while I was a student at IISc, Bangalore. I thank late Prof. P. Ramachandrarao (BHU, Varanasi), for inspiring me to think about the problem presented here, and the innumerable stimulating discussions. I also thank Archana Bhagyan for assistance with data analysis. I would like to dedicate this paper to late Prof. Robert Cahn for introducing me to the methodology of science.

Received 9 March 2009; revised accepted 12 August 2010

On acoustic theory of conch shell

Saroj Kumar Rath^{1,*} and P. C. Naik²

¹Department of Physics, Talcher College, Talcher 759 107, India

²Chhayapath Rural Research Centre, Nuagan, Post Kusiapal 754 250, India

We recently reported a study on the generation and resonance of sound in a shell assuming the straightened conch-cavity as a truncated horn. However, the tomographic picture reveals that the cavity grows as an Archimedes spiral carried forward in length. To account for the realistic case, in this study, the equation of propagation of sound waves in the shell is set up as Webster's horn equation in three dimensions in circular cylindrical coordinates. Solution of the angular and radial components of the equation on application of appropriate boundary conditions leads to an expression for frequency which is the same as the one reported earlier. However, solution of the z -component of the wave equation subjected to available boundary conditions poses the possibility of existence of very high frequency components, almost in the ultrasonic range. The intensity of radiation saturates in the high frequency range.

Keywords: Archimedes spiral, conch shell, ultrasonic component, Webster's horn equation.

THE conch shell is one of the earliest wind instruments found in nature. In view of its wide use as a musical instrument and trumpet by various cultures the world over through the ages and in view of the fact that little study has gone into its acoustics, we have taken up a close study of the system. In this process we reported the result of our study on morphology and tomographic pictures of the shell samples to show that the structure of the shell follows the Fibonacci pattern¹.

Further in a recent report we have presented our understanding of the mechanism of generation of musical sound in the conch shell². We have presented the sound spectra graphs from a number of shell samples produced on a computer using Spectra Plus software. The spectral characteristics have been observed and outlined. It has been pointed out that the shell sounds in 'lock-in' mode accompanied by frequencies of all integral multiples of the peak (i.e. lock-in) frequency.

In order to correlate the resonance frequency with the shell parameters, we have assumed the straightened shell cavity spiral to approximate a truncated horn. A well-known theory of conical horn has been applied, which leads to a frequency expression that agrees fairly well with the observed spectra.

However, as seen in the tomographic pictures, the conch cavity grows as an Archimedes' spiral carried

*For correspondence. (e-mail: sarojkrath@yahoo.co.in)

length-wise. Hence the truncated horn approximation is not a realistic description though it works well. Therefore in this study, a more realistic theory of propagation of sound in the shell has been developed by setting up the Webster's horn equation in three dimensions in circular cylindrical coordinates. Appropriate expression for the cavity cross-section was fed to the equation and the variables were separated. Solution of the angular and radial components of the equation, on application of appropriate boundary conditions with reasoning resulted in an expression for the resonance frequency which was the same as the one reported by our recent work².

It is interesting to note that the solution of z -component of the wave equation subject to the available boundary conditions offers the possibility of existence of frequency components in the 2 kHz range and their harmonics. This implies the conch sound possibly contains ultrasonic components. Further, the radiation pattern seems to saturate in the high frequency range. These results need to be tested in future experiments.

Webster's horn equation in one dimension is given by³⁻⁹

$$\ddot{\phi} = c^2 \frac{\partial^2 \phi}{\partial x^2} + c^2 \frac{\partial \phi}{\partial x} \cdot \frac{\partial (\ln S)}{\partial x}, \quad (1)$$

where ϕ is the velocity potential and S the area of cross-section of the path of sound propagation. We may generalize the equation as

$$\ddot{\phi} = c^2 \nabla^2 \phi + c^2 (\vec{\nabla} \phi) \cdot \vec{\nabla} (\ln S), \quad (2)$$

for the description of the conch where the cavity is wound around the collumella as a spiral both in the θ and z directions (Figure 1). Hence the circular cylindrical

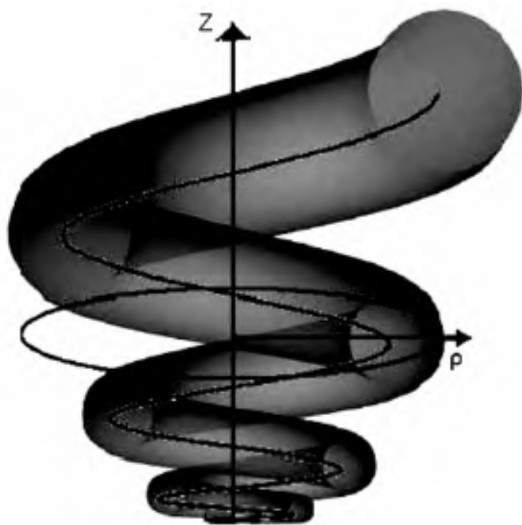


Figure 1. Schematic view of 3D growth of a conch spiral.

coordinates are the natural choice. Here the coordinates are (ρ, θ, z) . The measurement of parameters establishes the spiral to be Archimedes type with defining equation, $\rho = K\theta$ and the z -spiral growing as $\xi = kz$, where K and k are numerical parameters distinguishing the individual spirals. However, during the formalism these geometrical parameters drop out and the final conch equation appears independent of them.

In the $\rho\theta$ plane, the equations of two spirals bounding the inner and outer surfaces of the cavity are $\rho_1 = K_1\theta$, $\rho_2 = K_2\theta$, each value of K specifying a particular spiral. Let the central spiral be given by $\rho = \kappa\theta$, and the outer and the inner spirals by $\rho_1 = (\kappa - \lambda)\theta$ and $\rho_2 = (\kappa + \lambda)\theta$ respectively. So the diameter of cross-section in the $\rho\theta$ plane is $d = (\kappa + \lambda)\theta - (\kappa - \lambda)\theta = 2\lambda\theta$ and radius square = $\lambda^2\theta^2$. Similarly, in the z -direction, shift $dz = k'z$ and hence the inclined cross-section has a radius $r^2 = (\lambda\theta)^2 + (k'z)^2$. This leads to the expression for the cross-sectional area, assumed nearly circular as,

$$S = \lambda'\theta^2 + k'z^2, \quad (3)$$

where λ' and k' are constants. Therefore,

$$\ln S = \ln(\lambda'\theta^2 + k'z^2). \quad (4)$$

Let us consider Webster's horn equation in cylindrical coordinates.

Assuming $\phi(\rho, \theta, z, t) = \phi(\rho, \theta, z)e^{i\omega t}$, $\ddot{\phi} = -\omega^2 \phi(\rho, \theta, z, t)$. With this substitution, eq. (2) turns out to be,

$$\nabla^2 \phi + (\vec{\nabla} \phi) \cdot \vec{\nabla} (\ln S) = -\frac{\omega^2}{c^2} \phi. \quad (5)$$

Using standard expressions for ∇^2 and grad in circular cylindrical coordinates, eq. (5) turns out to be

$$\begin{aligned} -\frac{\omega^2}{c^2} \phi = & \left[\frac{1}{\rho} \frac{\partial}{\partial \rho} \left(\rho \frac{\partial}{\partial \rho} \right) + \frac{1}{\rho^2} \frac{\partial^2}{\partial \theta^2} + \frac{\partial^2}{\partial z^2} \right] \phi \\ & + \left(\hat{\rho} \frac{\partial \phi}{\partial \rho} + \hat{\theta} \frac{\partial \phi}{\partial \theta} + \hat{k} \frac{\partial \phi}{\partial z} \right) \cdot \left(\hat{\rho} \frac{\partial}{\partial \rho} + \hat{\theta} \frac{\partial}{\partial \theta} + \hat{k} \frac{\partial}{\partial z} \right) \\ & \times \{ \ln(\lambda\theta^2 + kz^2) \}. \end{aligned} \quad (6)$$

It may be noticed that $\ln S$ is independent of ρ and hence the ρ derivatives in the second term on RHS of eq. (6) do not contribute.

Upon effecting differentiation and dot product in the second term on RHS of eq. (6) we obtain,

$$\begin{aligned} -\frac{\omega^2}{c^2} \phi = & \left[\frac{1}{\rho} \frac{\partial}{\partial \rho} \left(\rho \frac{\partial}{\partial \rho} \right) + \frac{1}{\rho^2} \frac{\partial^2}{\partial \theta^2} + \frac{\partial^2}{\partial z^2} \right] \phi \\ & + \frac{1}{\rho^2} \left(\frac{\partial \phi}{\partial \theta} \right) \frac{2\lambda\theta}{(\lambda\theta^2 + kz^2)} + \left(\frac{\partial \phi}{\partial z} \right) \frac{2kz}{(\lambda\theta^2 + kz^2)}. \end{aligned} \quad (7)$$

Now we proceed to further simplify the last two terms on RHS above under certain approximation. The term $(\lambda\theta^2 + kz^2)$ in the denominator of the first term can be written as

$$\lambda\theta^2 + kz^2 = \lambda\theta^2 \left(1 + \frac{kz^2}{\lambda\theta^2} \right).$$

If $(kz^2/\lambda\theta^2) \ll 1$, i.e. spiral growth in the z -direction is much smaller than the growth in Θ , then $kz^2/\lambda\theta^2$ may be neglected and the complete first term gives

$$\frac{1}{\rho^2} \left(\frac{\partial \phi}{\partial \theta} \right) \frac{2}{\theta}. \quad (8)$$

However, under the same approximation, the second term reorganized as

$$\left(\frac{\partial \phi}{\partial z} \right) \cdot \left(\frac{2k}{z} \right) \left(\frac{1}{1 + \frac{\lambda\theta^2}{kz^2}} \right),$$

approaches zero and may be neglected.

Therefore, the wave equation will finally read,

$$\begin{aligned} \frac{1}{\rho} \frac{\partial}{\partial \rho} \left(\rho \frac{\partial \phi}{\partial \rho} \right) + \frac{1}{\rho^2} \frac{\partial^2 \phi}{\partial \theta^2} + \frac{\partial^2 \phi}{\partial z^2} \\ + \frac{1}{\rho^2} \left(\frac{\partial \phi}{\partial \theta} \right) \cdot \frac{2}{\theta} = -\frac{\omega^2}{c^2} \phi. \end{aligned} \quad (9)$$

Upon further simplification and rearrangement, the equation can be represented as

$$\begin{aligned} \frac{\partial^2 \phi}{\partial \rho^2} + \frac{1}{\rho} \frac{\partial \phi}{\partial \rho} + \frac{1}{\rho^2} \frac{\partial^2 \phi}{\partial \theta^2} + \frac{1}{\rho^2} \cdot \frac{2}{\theta} \cdot \frac{\partial \phi}{\partial \theta} \\ + \frac{\partial^2 \phi}{\partial z^2} + \frac{\omega^2}{c^2} \phi = 0. \end{aligned} \quad (10)$$

For solution of the wave equation, let us assume $\phi = P(\rho)\Psi(\theta)Z(z)$ as the product of functions of independent variables for their separation. Upon effecting the differentiations and dividing throughout by ϕ , one arrives at the equation,

$$\begin{aligned} \frac{1}{P} \frac{\partial^2 P}{\partial \rho^2} + \frac{1}{P} \frac{1}{\rho} \frac{\partial P}{\partial \rho} + \frac{1}{\rho^2 \Psi} \frac{\partial^2 \Psi}{\partial \theta^2} + \frac{1}{\rho^2} \frac{2}{\Psi \theta} \frac{\partial \Psi}{\partial \theta} \\ + \frac{1}{Z} \frac{\partial^2 Z}{\partial z^2} + \frac{\omega^2}{c^2} = 0. \end{aligned} \quad (11)$$

Let

$$\frac{1}{Z} \frac{\partial^2 Z}{\partial z^2} = -m^2, \quad (12)$$

which gives the immediate solution,

$$Z = e^{\pm imz}, \quad (13)$$

and eq. (11) turns to be,

$$\begin{aligned} \frac{1}{P} \frac{\partial^2 P}{\partial \rho^2} + \frac{1}{P\rho} \frac{\partial P}{\partial \rho} + \frac{1}{\rho^2 \Psi} \frac{\partial^2 \Psi}{\partial \theta^2} + \frac{1}{\rho^2} \frac{2}{\Psi \theta} \frac{\partial \Psi}{\partial \theta} \\ + \left(\frac{\omega^2}{c^2} - m^2 \right) = 0. \end{aligned} \quad (14)$$

Let us again assume

$$\left(\frac{\omega^2}{c^2} - m^2 \right) = \gamma^2. \quad (15)$$

With this substitution, eq. (14) now reads,

$$\frac{1}{P} \frac{\partial^2 P}{\partial \rho^2} + \frac{1}{P\rho} \frac{\partial P}{\partial \rho} + \frac{1}{\rho^2 \Psi} \frac{\partial^2 \Psi}{\partial \theta^2} + \frac{1}{\rho^2} \frac{2}{\Psi \theta} \frac{\partial \Psi}{\partial \theta} + \gamma^2 = 0. \quad (16)$$

Multiplying by ρ^2 throughout,

$$\frac{\rho^2}{P} \frac{\partial^2 P}{\partial \rho^2} + \frac{\rho}{P} \frac{\partial P}{\partial \rho} + \frac{1}{\Psi} \frac{\partial^2 \Psi}{\partial \theta^2} + \frac{1}{\Psi} \frac{2}{\theta} \frac{\partial \Psi}{\partial \theta} + \gamma^2 \rho^2 = 0. \quad (17)$$

Assuming

$$\frac{1}{\Psi} \frac{\partial^2 \Psi}{\partial \theta^2} + \frac{2}{\theta \Psi} \frac{\partial \Psi}{\partial \theta} = -\alpha^2,$$

a constant, the equation turns to be

$$\frac{\partial^2 \Psi}{\partial \theta^2} + \frac{2}{\theta} \frac{\partial \Psi}{\partial \theta} + \alpha^2 \Psi = 0. \quad (18)$$

This is an equation in standard form, which can be reduced to normal form using the standard technique to provide the solution

$$\Psi = \frac{e^{\pm i\alpha\theta}}{\theta}. \quad (19)$$

Now the radial equation to be solved reads,

$$\rho^2 \frac{\partial^2 P}{\partial \rho^2} + \frac{\rho}{P} \frac{\partial P}{\partial \rho} + (\gamma^2 \rho^2 - \alpha^2) = 0,$$

or

$$\rho^2 \frac{\partial^2 P}{\partial \rho^2} + \rho \frac{\partial P}{\partial \rho} + (\gamma^2 \rho^2 - \alpha^2) P = 0. \quad (20)$$

This is Bessel equation with argument $\gamma\rho$. It may be noticed that the equation is free of conch parameters, K and k . Equation (20) has Bessel functions of order α , i.e. $J_\alpha(\gamma\rho)$ as its solution. Hence the complete solution, including time dependence is given by

$$\phi = A J_\alpha(\rho\gamma) \frac{e^{\pm i\alpha\theta}}{\theta} e^{\pm i n \pi} e^{i\alpha}, \quad (21)$$

where A is a constant of integration.

In order to match the solution with physical parameters of the conch shell, we now apply boundary conditions on acoustic impedance of the system.

By definition

$$\mathbb{Z} = \frac{P}{S \dot{\xi}}, \quad (22)$$

where P is given by

$$P = \sigma \dot{\phi} = i\omega\sigma\phi, \quad (23)$$

where σ is the density.

Therefore,

$$\mathbb{Z} = \frac{i\omega\sigma\phi}{S \dot{\xi}}. \quad (24)$$

At the open end, $\dot{\xi}$ being the velocity is non-zero and impedance is 0. This implies that ϕ vanishes. But since ϕ is a product of three independent functions, each of them simultaneously must be zero.

One may take the z and θ solutions. The most general z solution can be written as

$$z = a_m \cos mz + b_m \sin mz. \quad (25)$$

Taking $a_m = 0$, z vanishes at $z = z_l$,

$$\text{if } \sin(mz_l) = 0 \Rightarrow mz_l = n\pi,$$

$$\text{or } m = \frac{n\pi}{z_l}, \quad \text{where } n = 0, \pm 1, \pm 2, \pm 3, \dots \quad (26)$$

Similarly, the θ function, i.e. $\Psi(\theta)$ vanishes when

$$\sin \alpha\theta = 0 \Rightarrow \alpha\theta = P\pi$$

$$\text{or } \alpha = \frac{P\pi}{\theta}, \quad \text{where } P = 0, 1, 2, 3, \dots$$

But for the shell, $\theta = 8\pi$ on completion of four turns.

$$\text{So } \alpha = \frac{P}{8}. \quad (27)$$

Finally let us consider the condition of the Bessel function vanishing at $\rho = a$, where a is the final radius of the spiral. Now from the defining relation, eq. (15),

$$\frac{\omega}{c} = \sqrt{\gamma^2 + m^2} = \sqrt{\gamma^2 + \frac{n^2 \pi^2}{z_l^2}}. \quad (28)$$

It may be noticed that, putting $n = 0$, suppresses the frequency component due to linear growth and limits ω/c to γ only.

Again from eq. (21), $J_\alpha(\rho\gamma) = 0$ at $\rho = a$. So $J_\alpha(\gamma a) = 0$. Assuming $p = 1$, $\alpha = 1/8$.

But the values of γa for zeros of $J_{1/8}$ will never give harmonics and hence are not the correct solution for the conch shell. The only harmonics solutions are possible for $\alpha = 1/2$, i.e. for $p = 4$ in eq. (26). It is known that

$$J_{1/2}(\gamma a) = \frac{1}{\sqrt{\pi\gamma a}} \sin(\gamma a),$$

and its zeroes occur at $\gamma a = \tau\pi$, $\tau = 0, 1, 2, 3, \dots$

$$\text{For } \tau = 1, \gamma a = \pi, \gamma = \frac{\pi}{a},$$

$$\text{or } \frac{\omega}{c} = \frac{\pi}{a},$$

$$\text{or } f = \frac{c}{2a}. \quad (29)$$

Further, a factor of $\sqrt{2}$ comes from double the volume with reference to Figure 2 and the explanation that follows later and is to be multiplied in the denominator to

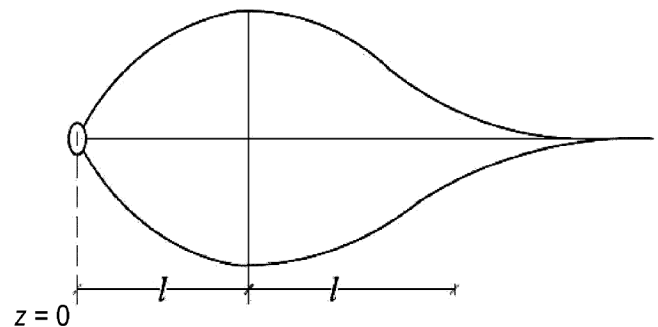


Figure 2. External geometry of the conch shell.

give the final frequency formula in terms of the conch radius as

$$f = \frac{c}{2\sqrt{2}a}. \quad (30)$$

But in the case of the conch spiral the radius vector a is not reached by the disturbance continuously. It comes in successive steps in the spiral growth and hence takes the same time as the disturbance takes to travel from the apex to the mouth. So the effective radial distance is the length of the spiral, which turns out to be $L = 4\pi\sqrt{2}a$. Therefore replacing a by $4\pi\sqrt{2}a$ we get the final frequency formula

$$f = \frac{c}{16\pi a}. \quad (31)$$

It has been demonstrated earlier by us¹ that the eq. (31) agrees fairly well with experiments in providing fundamental frequencies of samples of the conch shell.

Let us now look into the actual conch geometry. If $2l$ is the length of the shell, its radius grows up to approximately length l and then onwards it gradually reduces shaping the other half of the shell almost in the form of a cone (Figure 2). In Figure 3 we present such a cone and consider propagation of sound from the cone mouth towards its apex. The sectional area of the cone at any z is given by

$$S_e = \pi \tan^2 \Theta \cdot (l-z)^2,$$

where Θ is the constant angle of the cone.

One can rewrite the Webster's horn equation for this particular case to arrive at

$$-\frac{\omega^2}{c^2} = \frac{\partial^2 \phi}{\partial z^2} + \frac{\partial \phi}{\partial z} \cdot \frac{\partial}{\partial z} (\ln S) = \frac{\partial^2 \phi}{\partial z^2} + \frac{\partial \phi}{\partial z} \cdot \frac{2}{(z-l)}. \quad (32)$$

$$\text{Let } z-l = \zeta \Rightarrow dz = d\zeta.$$

With this substitution, the wave equation, i.e. eq. (32) will be

$$-\frac{\omega^2}{c^2} = \frac{\partial^2 \phi}{\partial \zeta^2} + \frac{\partial \phi}{\partial \zeta} \cdot \frac{2}{\zeta} \quad (33)$$

with the solution,

$$\phi = \frac{e^{\pm i \frac{\omega}{c} (-z+l)}}{(z-l)}.$$

Upon application of the condition of openness at $z = l_0$, we get

$$\frac{\omega}{c} \cdot (l-l_0) = \pm n\pi, \text{ or } \omega = \frac{nc\pi}{(l-l_0)}, \quad (34)$$

$$\text{or } f = \frac{nc}{2(l-l_0)}. \quad (35)$$

For z very close to l , say $l-l_0 = 1 \text{ cm} = 0.01 \text{ m}$,

$$f_z = \frac{345}{2 \times 0.01} = \frac{345}{0.02} = 17,250 \text{ Hz}$$

and the subsequent harmonics are all above the ultrasonic range of 20,000 Hz. Hence, in a way, the theory predicts the possibility of existence of ultrasonic component of sound in the conch notes.

We apply radiation intensity formula here as appropriate for a conical horn. It is pertinent to point out here that for the conch shell, the solution for velocity potential appears as the product of three independent functions, p , ψ and Z . However, the frequency dependence of the intensity may be ensured out of the z -component only, when it is taken as

$$\phi = \frac{A}{\Omega z} e^{i(\omega t - kz)}, \quad (36)$$

where Ω is the solid angle open for radiation.

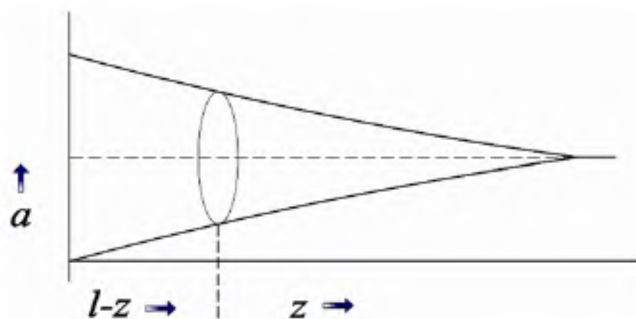


Figure 3. Lower half structure of a conch shell.

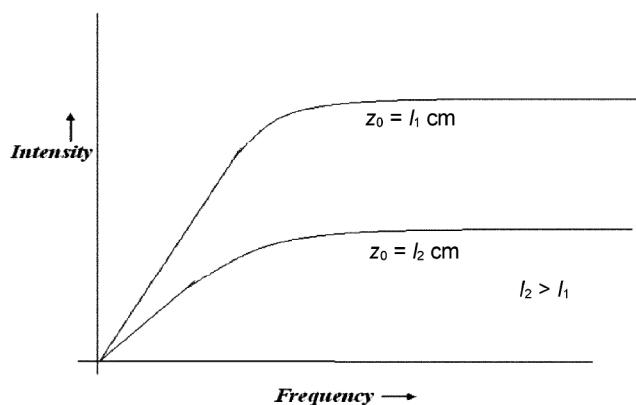


Figure 4. Frequency-intensity curve.

With usual argument and redoing all steps as described in standard texts^{3,5} for a conical horn, the radiation intensity is given by

$$\frac{dw}{dt} = \frac{p_{\max}^2}{2\sigma c} = \frac{A^2 \sigma c}{2s\Omega} \frac{k^2}{(1+k^2 z_0^2)}, \quad (37)$$

where z_0 is a point in the z -direction from the lower apex of the shell, where the opening of the mouth piece is located. The frequency–intensity curve as indicated by the theory is given in Figure 4.

It may be noticed that for the conch shell, $l - z_0$ is very small, may be of the order of less than 1 cm. In this case the response may be steep and the intensity may be uniform for all higher frequencies. This predicts that the ultrasonic frequencies and their overtones, if at all present, will appear with almost uniform intensity.

In this communication, we have presented the problem of propagation of sound waves in the coiled tunnel of a conch shell cavity; set up the Webster's horn equation in circular cylindrical coordinates and solved them. The solutions with application of proper boundary conditions, and physical situation, offer expressions for frequency, which computed with the conch parameters give the correct match with the observed frequency. Existence of the ultrasonic component in the conch spectrum is indicated by the theory. The theory further points out uniform intensity distribution for such high frequency components.

1. Rath, S. K. and Naik, P. C., Fibonacci structure in conch shell. *Curr. Sci.*, 2005, **88**, 555–557.
2. Rath, S. K. and Naik, P. C., A study on acoustics of conch shell. *Curr. Sci.*, 2009, **97**, 521–528.
3. Wood, A., *Acoustic*, Blackie & Son Limited, London, 1910, 1st edn, pp. 115–118.
4. Morse, P. M., *Vibration and Sound*, McGraw Hill, Tokyo, 1948, 2nd edn, p. 269.
5. Crandall, I. B., *Vibrating System and Sound*, Macmillan & Co Ltd, 1927, pp. 153–155.
6. Fletcher, N. and Rossing, T. D., *The Physics of Musical Instrument*, Springer Verlag, New York, 1991, p. 188.
7. Rienstra, S. W., Webster's horn equation revisited. *J. Appl. Math.*, 2004, **65**(6), 1981–2004.
8. Eisner, E., Complete solution of the 'Webster horn equation'. *J. Acoust. Soc. Am.*, 1967, **41**(4B), 1126–1147.
9. Martin, P. A., On Webster's horn equation and some generalizations. *J. Acoust. Soc. Am.*, 2004, **116**(3), 1382–1388.

ACKNOWLEDGEMENTS. We thank Dr P. S. Naik, University of Hong Kong, Hong Kong for help in providing information and literature, during the course of this work. We also thank Rudra Sabitru Nayak, Rythm Architects Pvt Ltd, Bhubaneswar, for help in drawing figures.

Received 12 February 2010; accepted 16 August 2010

Studies on Makhana (*Euryale ferox* Salisbury)

Arvind Kumar Verma¹, B. K. Banerji¹,
Debasis Chakrabarty¹ and S. K. Datta^{2,*}

¹National Botanical Research Institute (CSIR), Rana Pratap Marg, Lucknow 226 001, India

²Bose Institute, Madhyamgram Experimental Farm, Jessore Road, 24 Parganas (N), Kolkata 700 129, India

Makhana (*Euryale ferox* Salisbury) grows as an exclusive aquatic cash crop in shallow water bodies in north Bihar and lower Assam regions of India. It has nutritional and medicinal properties and supports cottage industry. It is a monotypic genus and the available genetic variability is limited. An attempt was made to understand the cultural practices, genetic variability among the available germplasm and the biochemical changes during seed germination. It was included in an improvement programme using gamma ray induced mutagenesis. Different morphological parameters were selected to find out its sensitivity to different doses of gamma rays.

Keywords: Makhana, gamma rays, monotypic, mutation.

EURYALE FEROX Salisbury (Nymphaeaceae), known as Makhana, is distributed in tropical and subtropical regions of south-east and east Asia. It grows as an exclusive aquatic cash crop in shallow water bodies in north Bihar and lower Assam regions of India. It has nutritional and medicinal properties and supports cottage industry. It is cultivated in ponds, lakes, tanks and other aquatic bodies. Distribution, ecology, agronomy, biology, pests, production and processing of Makhana have been compiled earlier¹. The major drawback with Makhana cultivation is that the interlacing ribs of leaves and petioles are prickly. The mature fruits are borne on long pedicels and are difficult to harvest due to the stout prickles on the outer surface. Makhana is a monotypic genus and the available genetic variability is limited. Although it is an important aquatic crop, work on its improvement was not initiated earlier using the conventional breeding and induced mutagenesis techniques. Because it is a monotypic genus, induced mutagenesis is the best available method for its improvement. An attempt was made to test the sensitivity of Makhana to physical mutagen and to induce desirable genetic variability (spineless strain, new better varieties, early flowering/early maturity strains, high yielding variety with increased seed number, increased seed weight, increased seed size, increased fruit number, increased floral stalk, increased berry size, etc.) through induced mutagenesis.

*For correspondence. (e-mail: subodhskdatta@rediffmail.com)